



HAL
open science

Influence of Ce^{3+} ion on optical properties and radiation resistance in Ce^{3+}/Tm^{3+} -co-doped alumino-silicate glasses

Yan Jiao, Chongyun Shao, Mengting Guo, Malgorzata Guzik, Yang Zhang, Chunlei Yu, Georges Boulon, Lili Hu

► **To cite this version:**

Yan Jiao, Chongyun Shao, Mengting Guo, Malgorzata Guzik, Yang Zhang, et al.. Influence of Ce^{3+} ion on optical properties and radiation resistance in Ce^{3+}/Tm^{3+} -co-doped alumino-silicate glasses. *Optical Materials: X*, 2022, 13, pp.100113. 10.1016/j.omx.2021.100113. hal-03715235

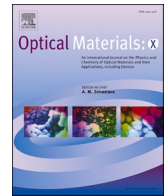
HAL Id: hal-03715235

<https://hal.science/hal-03715235>

Submitted on 6 Jul 2022

HAL is a multi-disciplinary open access archive for the deposit and dissemination of scientific research documents, whether they are published or not. The documents may come from teaching and research institutions in France or abroad, or from public or private research centers.

L'archive ouverte pluridisciplinaire **HAL**, est destinée au dépôt et à la diffusion de documents scientifiques de niveau recherche, publiés ou non, émanant des établissements d'enseignement et de recherche français ou étrangers, des laboratoires publics ou privés.



Influence of Ce³⁺ ion on optical properties and radiation resistance in Ce³⁺/Tm³⁺-co-doped alumino-silicate glasses

Yan Jiao^{a,b}, Chongyun Shao^a, Mengting Guo^{a,b}, Malgorzata Guzik^c, Yang Zhang^d, Chunlei Yu^{a,e}, Georges Boulon^{f,**}, Lili Hu^{a,e,*}

^a Key Laboratory of Materials for High Power Laser, Shanghai Institute of Optics and Fine Mechanics, Chinese Academy of Sciences, Shanghai, 201800, PR China

^b Center of Materials Science and Optoelectronics Engineering, University of Chinese Academy of Sciences, Beijing, 100049, PR China

^c Faculty of Chemistry, University of Wrocław, ul. F. Joliot-Curie 14, 50-383, Wrocław, Poland

^d Shanghai Institute of Satellite Engineering, Shanghai, 201109, PR China

^e Hangzhou Institute for Advanced Study, University of Chinese Academy of Sciences, Hangzhou, 310024, PR China

^f Institute Light Matter (iLM), UMR 5306 UCB Lyon 1-CNRS, University of Lyon, 69622, Villeurbanne, France

ARTICLE INFO

Keywords:

Alumino-silicate glasses
Ce³⁺/Tm³⁺ ions
Sol-gel method
Optical materials
Radiation resistance

ABSTRACT

Several Ce³⁺/Tm³⁺-co-doped alumino-silicate glasses with various Ce³⁺/Tm³⁺ ratios were prepared by a sol-gel method combined with vacuum sintering. To determine their radiation resistance, the glasses were exposed to 1 and 100 kGy γ -ray. The effect of the Ce³⁺/Tm³⁺ ratio on the absorption, emission and fluorescence lifetime of the glasses under investigation, was examined before and after irradiation. The Ce⁴⁺ and Ce³⁺ cations were detected and the nature of Si-E' and ALOHC color centers caused by irradiation was identified by radiation-induced absorption (RIA) and electron paramagnetic resonance (EPR) spectroscopy. Co-doping with Ce³⁺ ions can significantly improve the radiation resistance of the glass, although it can deteriorate the spectral properties of Tm³⁺ ions. Additionally, the related influence mechanisms are discussed. The obtained results indicate that Ce³⁺/Tm³⁺-co-doped alumino-silicate glasses with optimized Ce³⁺ ion concentrations, a Ce³⁺/Tm³⁺ molar ratio less than 0.3, can be used as an active medium for radiation-resistant materials in harsh radiation environments.

1. Introduction

Over the past decades, Tm³⁺-doped silica fiber (TDF) lasers and amplifiers attracted considerable attention, owing to their high efficiency, excellent beam quality, perfect reliability and favorable atmospheric transmission window, and broad application prospects [1–7]. Moreover, TDF has been utilized in harsh radiation environments, such as deep space exploration and laser communication, military conflicts [2,3,6], and other fields. However, exposing TDFs to high-energy radiation (X-rays, γ -rays or protons) generates a higher radiation-induced absorption (RIA) compared to passive fibers (pure silica) [8]. This is mainly attributed to the addition of Al³⁺, P⁵⁺, Ge⁴⁺ ions and/or other elements in the active fiber, which reportedly reduces the clustering of rare-earth (RE) ions and improves the performance of fiber-based amplifiers or lasers [9]. In addition, the elements generate color centers and a remarkable additional attenuation of glass-based fiber [10]. However,

color centers are largely responsible for the degradation of optical properties, and strongly affect the quantum yield and operating lifetime [11–13]. Therefore, the fundamental goal of improving the radiation resistance of optical fibers is to prevent the formation of color centers.

Considerable efforts have been devoted to enhancing the radiation resistance of silica glasses and fibers. The general methodology is to optimize the core composition as well as the pre- and post-treatment conditions of the fiber. Composition optimization mainly refers to co-doping Ce³⁺ and/or F⁻ ions into the fiber core [14]. Pre-treatment generally involves pre-loading H₂ or D₂, or pre-irradiating, or pre-annealing the non-irradiated optical fiber, to improve its radiation resistance [15–17]. Post-treatment generally entails photobleaching or thermal bleaching the irradiated optical fiber, to reduce its RIA level [13,18]. Although effective, there are some disadvantages of these methods, namely the gas out-diffusion in the H₂ or D₂ loaded optical fiber [19] and the limited improved radiation resistance of

* Corresponding author. Key Laboratory of Materials for High Power Laser, Shanghai Institute of Optics and Fine Mechanics, Chinese Academy of Sciences, Shanghai, 201800, PR China.

** Corresponding author. Institute Light Matter (iLM), UMR 5306 UCB Lyon 1-CNRS, University of Lyon, 69622, Villeurbanne, France

E-mail addresses: georges.boulon@univ-lyon1.fr (G. Boulon), hulili@siom.ac.cn (L. Hu).

<https://doi.org/10.1016/j.omx.2021.100113>

Received 11 June 2021; Received in revised form 16 October 2021; Accepted 2 November 2021

Available online 12 November 2021

2590-1478/© 2021 The Authors.

Published by Elsevier B.V. This is an open access article under the CC BY-NC-ND license

(<http://creativecommons.org/licenses/by-nc-nd/4.0/>).

Table 1
Mean composition of glass samples.

Sample name	Al ₂ O ₃ (mol. %)	Tm ₂ O ₃ (mol. %)	Ce ₂ O ₃ (mol. %)	Ce/Tm ratio
1A1	1	0	0	–
TAC0	1	0.1	0	0
TAC3	1	0.1	0.03	0.3
TAC6	1	0.1	0.06	0.6
TAC9	1	0.1	0.09	0.9
TAC12	1	0.1	0.12	1.2

pre-irradiated or pre-annealed active fibers which could partially destroy the coating of the optical fiber [20]. In addition, the conventional post-processing method is incapable of completely eliminating the RIA of the darkened fiber due to the poor temperature resistance of the polymer-based coating [21].

Some researchers have attempted to improve the radiation resistance of Tm³⁺-doped glasses and optical fibers under γ -ray irradiation. Others studies reported the influence of loading H₂ or D₂ [22] and pump bleaching [23] on the radiation resistance of TDF. Compared with these pre-treatment and post-treatment, co-doping with cerium proposed as a superior alternative to improve the radiation resistance of TDF.

Recently, Ce³⁺-co-doping was shown to be a very effective method for reducing the radiation sensitivity of Er³⁺/Yb³⁺-co-doped [24] and Yb³⁺-doped fibers and amplifiers [25] without diminishing the amplification efficiency. The Ce³⁺ and Ce⁴⁺ ions coexist in these optical glasses and fibers. The Ce³⁺ ions can trap the radiation-induced holes to convert into Ce⁴⁺, thereby suppressing the formation of other centers. The Ce⁴⁺ ions inhibit the formation of the center generated by trapped electrons, which prevents the formation of color centers absorbed in the ultraviolet-visible (UV-Vis) range [26]. However, to the best of our knowledge, this study is the first to explore the influence of Ce³⁺-doping on the radiation resistance and spectral properties of Tm³⁺-doped silica glass and/or fiber.

In this work, Ce³⁺/Tm³⁺-co-doped aluminosilicate glasses with different Ce₂O₃ contents were prepared by a sol-gel method combined with vacuum sintering. The influence of Ce₂O₃ content on the spectroscopic properties was compared before and after γ -ray irradiation. The

aim of this work was to optimize the doping content of Ce₂O₃ and to elucidate the nature of color centers appearing in the aluminosilicate glasses. The radiation-induced color centers were systematically studied using EPR and absorption spectroscopy. These results will contribute to the development of TDFs utilized in harsh radiation environments.

2. Experimental

2.1. Glass preparation

The 0.1Tm₂O₃-1Al₂O₃-xCe₂O₃-(98.9-x)SiO₂ glasses (in mol%, x = 0, 0.03, 0.06, 0.09, 0.12) shown in Table 1 were prepared by the sol-gel method combined with vacuum sintering. Based on the Ce³⁺/Tm³⁺ molar ratio, the glasses are either classified as TACn (n = 0, 3, 6, 9 and 12) or they are more broadly referred to as the TAC glasses. In addition, Al³⁺ single-doped glass (1A1) was also prepared by the same method. The details of the preparation process are provided in Ref. [27]. Tetraethoxysilane (TEOS), C₂H₅OH, AlCl₃·6H₂O (Aladdin, 99.99%), TmCl₃·6H₂O (Aladdin, 99.99%), and CeCl₃·7H₂O (Aladdin, 99.99%) were used as precursors, whereas ethanol was used as the solvent and deionized water was added to sustain the hydrolysis reaction. The above-mentioned analytically pure grade chemical reagents were mixed and stirred for 24 h at room temperature (~25 °C) to form a homogeneous and clear doping gel. To decompose the organic matter and hydroxyl groups, the gel was heated in the oxygen atmosphere from 70 °C to 1100 °C, during which some of the Ce³⁺ ions were oxidized to Ce⁴⁺ ions. The resulting powder was placed in an alumina crucible and sintered at 1750 °C for 2 h under vacuum. Inductively coupled plasma atomic emission spectroscopy (ICP-AES) indicated that the Tm₂O₃, Al₂O₃, and Ce₂O₃ contents in these aluminosilicate glasses were close to the theoretical values.

To study the effect of γ -ray irradiation on the optical and spectroscopic properties of the Ce³⁺/Tm³⁺-co-doped aluminosilicate glasses, each glass was cut into two pieces: the one piece was exposed to γ -ray, and the other used as a reference. The glasses were exposed to γ -ray from a ⁶⁰Co γ -source under normal atmosphere up to total doses of 1 kGy and 100 kGy at a dose rate of 59 Gy/h and 5900 Gy/h. The bulk glasses were then polished to a thickness of 1 mm for the optical property

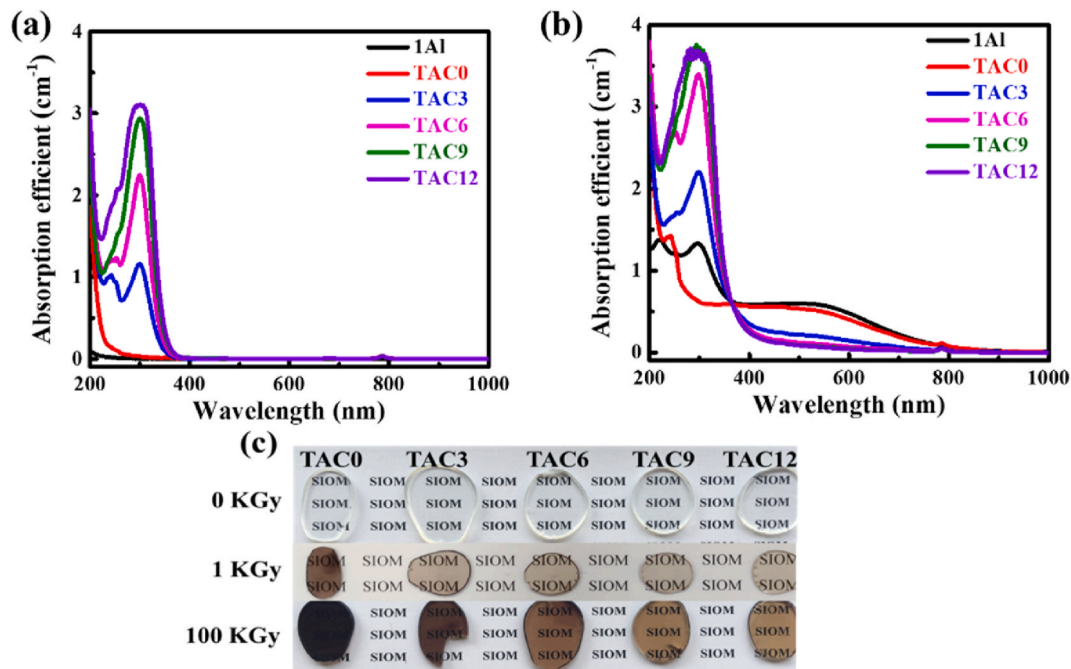


Fig. 1. Absorption spectra of the TAC aluminosilicate glasses (a) before and (b) after 1 kGy γ -ray irradiation. (c) Photography of the TAC aluminosilicate glasses before and after irradiation.

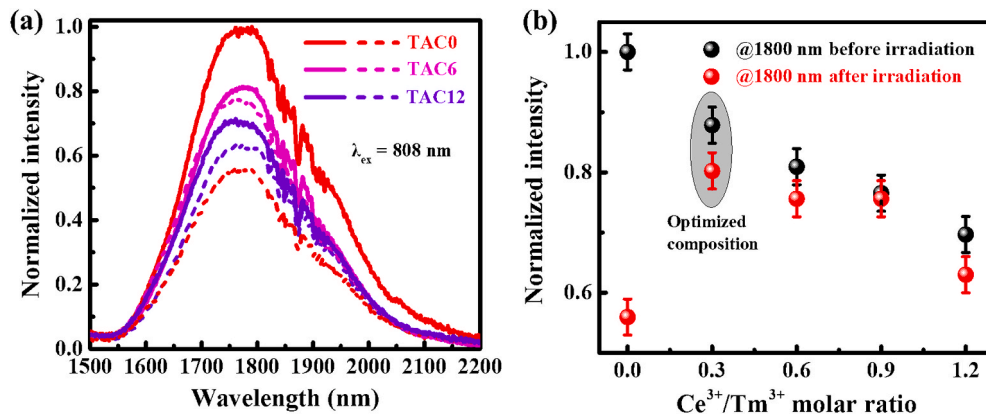


Fig. 2. (a) Fluorescence spectra of the TAC alumino-silicate glasses before (solid curve) and after (dash curve) 100 kGy γ -ray irradiation measured under excitation of $\lambda_{ex} = 808$ nm aser diode; (b) The luminescence intensity of the Tm^{3+} ion at approximately 1800 nm as a function of the Ce^{3+}/Tm^{3+} molar ratio.

measurements.

2.2. Apparatus

The absorption spectra were recorded using a PerkinElmer Lambda 900 UV/VIS/NIR spectrophotometer in the range of 190–2100 nm. The emission spectra, excited by an 808 nm laser diode, were detected using an Edinburg FLS 920 spectrometer. The fluorescence lifetime was measured via pulsed 808 nm optical parametric oscillation (OPO) laser excitation with an FLS 920.

EPR measurements for paramagnetic point defects were performed at room temperature on a Bruker ELEXSYS-II E500 CW-EPR spectrometer operating at the X band (9.38 GHz) in the 325–345 mT magnetic field range with 1-mW microwave power. All the EPR spectra were normalized to the same receiver gain. The powdered samples of approximately 100 mg were used for the EPR tests.

3. Results and discussion

3.1. Changes in absorption and emission spectra caused by irradiation

Fig. 1(a) and (b) shows the absorption spectra of TAC glasses before and after 1 kGy γ -ray irradiation. For a visual comparison, Fig. 1(c) shows the photography of TAC alumino-silicate glasses before and after irradiation with a dose of 1 kGy and 100 kGy.

Before irradiation, the TAC0 glass had noticeable absorption from the visible to the near-infrared region compared with the 1Al glass, due to the absorption of Tm^{3+} ions (Fig. 1(a)). For the Ce^{3+}/Tm^{3+} -co-doped

alumino-silicate glasses, a strong and broad absorption band was observed in the UV region that extend into the visible region (400 nm). This absorption range is assigned to the superposition of the absorption edge of the pure silica glass (~ 190 nm), charge transfer (CT) transitions (~ 260 nm) of Ce^{4+} from the oxygen orbitals of the valence band to the Ce orbitals, and the first $4f^1 \rightarrow 4f5d^1$ transitions of Ce^{3+} (302 nm) [28]. The assignment of the 260 and 302 nm absorption bands agrees with that of Ce^{4+} and Ce^{3+} -co-doped crystal scintillators, considering the energy shift corresponds to the difference between the nature of crystals and glasses [29,30].

After 1 kGy γ -ray irradiation (since the signal was saturated, the absorption of the samples after irradiation of 100 kGy is not shown here), the absorption coefficients significantly increase in the UV and visible regions compared with the same glasses before irradiation, and the degree of change in absorption gradually increases as the wavelength decreases. The 1Al and Tm^{3+} -doped alumino-silicate glass (TAC0) have highest additional absorption in the UV and visible regions, as shown in Fig. 1(b). This means that Ce free samples have the worst radiation resistance properties. As shown in Fig. 1(c), the extent of color darkening after radiation decreases with increasing Ce^{3+}/Tm^{3+} , which suggests that the radiation resistance significantly improved with an increase in the cerium ion concentration.

Fig. 2(a) demonstrates the normalized photoluminescence (PL) intensity of the ${}^3H_4 \rightarrow {}^3H_6$ transition of Tm^{3+} ions in the typical glasses (TAC0, TAC6 and TAC12) before and after 100 kGy γ -ray irradiation measured by excitation with an 808 nm laser diode. For comparison, all spectra were divided by the maximum intensity at 1800 nm for the un-irradiated TAC0 glass. In the pristine TAC glasses, the PL intensity was

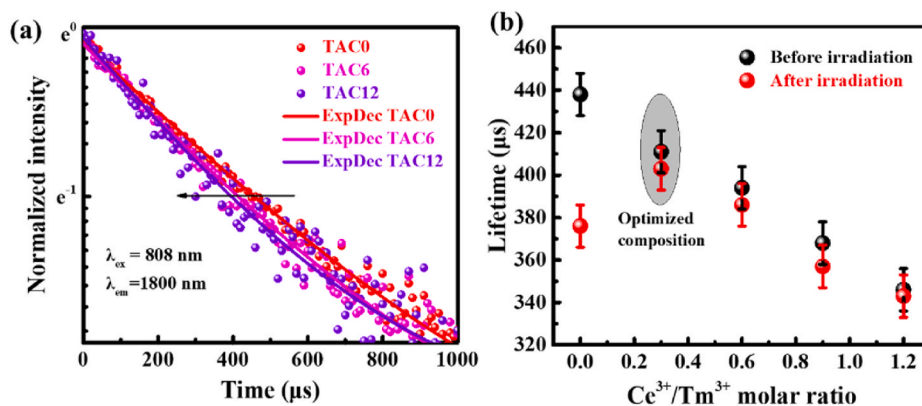


Fig. 3. (a) Decay curves of the 3F_4 excited state of Tm^{3+} ions from the ${}^3F_4 \rightarrow {}^3H_6$ emission transition (1800 nm) under pumping into 3H_4 (808 nm) in the TAC glasses with different Ce^{3+}/Tm^{3+} ratios before irradiation. (b) 3F_4 excited state lifetime values of Tm^{3+} before and after 100 kGy irradiation as a function of the Ce^{3+}/Tm^{3+} molar ratio.

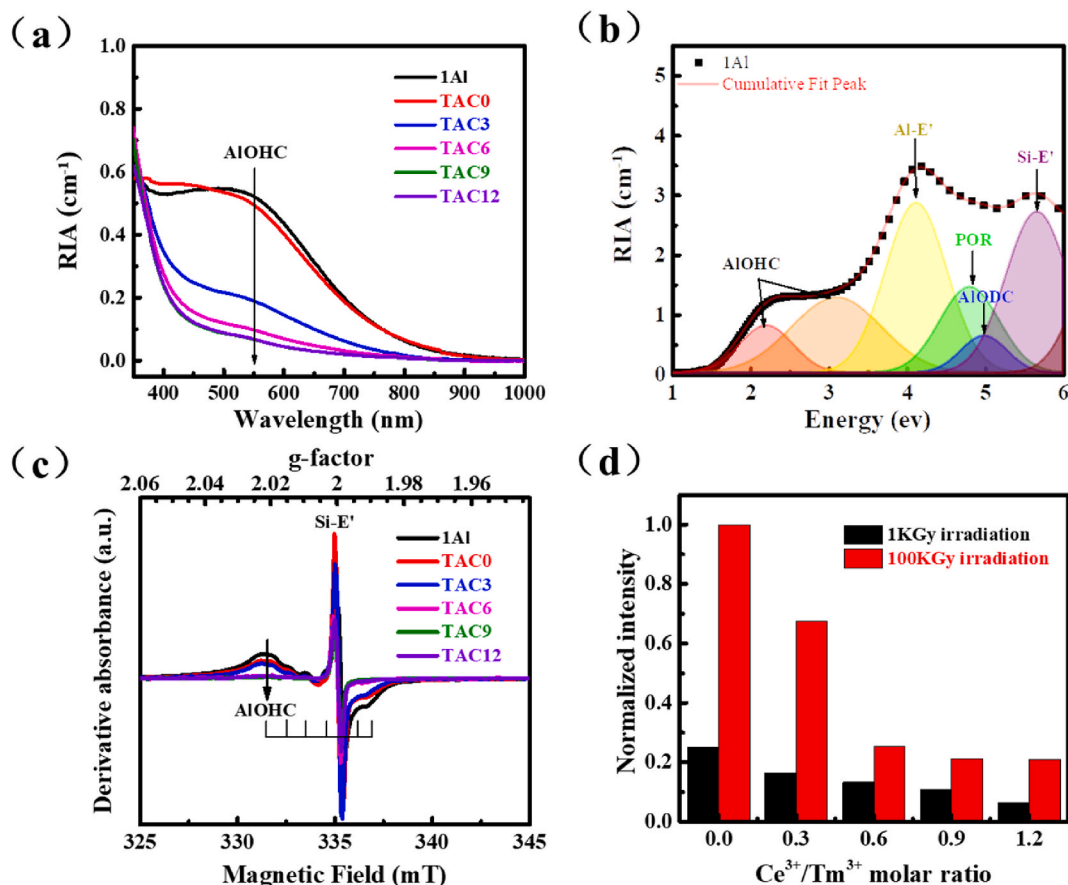


Fig. 4. (a) RIA spectrum of the TAC glasses, (b) Gaussian decomposition of the RIA spectrum of the 1Al glass, (c) EPR spectra (300 K) of 1 kGy γ -ray irradiated TAC glasses, (d) normalized double integration intensity of defects as a function of the $\text{Ce}^{3+}/\text{Tm}^{3+}$ molar ratio.

significantly quenched with an increase in the $\text{Ce}^{3+}/\text{Tm}^{3+}$ ratio. After γ -ray irradiation, the PL intensity of all TAC glasses decreased. Notably, the PL intensity of the TAC12 glass was only 60% of that of the TAC0 glass without Ce doping.

To examine the effect of γ -ray irradiation, Fig. 2(b) shows the PL intensity of the TAC glasses as a function of the $\text{Ce}^{3+}/\text{Tm}^{3+}$ ratio before and after 100 kGy λ -ray irradiation (at ~ 1800 nm). Before irradiation, the PL intensity of the TAC glasses was significantly quenched with an increase in the $\text{Ce}^{3+}/\text{Tm}^{3+}$ ratio. After irradiation, the PL intensity of TAC0 declined significantly although the reduction in intensity was effectively suppressed as the $\text{Ce}^{3+}/\text{Tm}^{3+}$ ratio increased. Moreover, the change in the PL intensity gradually decreased as the $\text{Ce}^{3+}/\text{Tm}^{3+}$ ratio increased. For the TAC6 glass, there was minimal change in the PL intensity before and after irradiation. This suggests that co-doping with Ce_2O_3 can greatly improve the radiation resistance of the TAC glasses.

Fig. 3(a) illustrates the effect of $\text{Ce}^{3+}/\text{Tm}^{3+}$ ratio on the decay profiles of the excited state of Tm^{3+} ions from the ${}^3\text{F}_4 \rightarrow {}^3\text{H}_6$ emission transition (1800 nm) under pumping into ${}^3\text{H}_4$ (808 nm, by an OPO pulsed laser) for the samples before irradiation. All curves were fitted by single exponential decay, and the fitted lifetime values were shown in Fig. 3(b). The lifetimes of the typical glasses are 438 μs (TAC0), 394 μs (TAC6), and 346 μs (TAC12). With increasing of $\text{Ce}^{3+}/\text{Tm}^{3+}$ ratio, the decay time drastically decreased. This is due to the energy transfer between the Tm^{3+} and Ce^{3+} ions, which quenches the ${}^3\text{H}_4 \rightarrow {}^3\text{H}_6$ emission transition of Tm^{3+} ions (see Section 3.3). A similar phenomenon was reported by Basiev et al. with the quenching of Tm^{3+} ions by Ce^{3+} ions in a two-particle cooperative acceptor [31].

Fig. 3(b) presents the excited state lifetime values of Tm^{3+} in the TAC glasses as a function of the $\text{Ce}^{3+}/\text{Tm}^{3+}$ ratio, before and after 100 kGy irradiation. After irradiation, the lifetime for the glass without the Ce^{3+}

ion (TAC0) was significantly quenched from 438 μs to 376 μs . This behavior is correlated with the RIA, due to the interaction between the Tm^{3+} ions and point defects produced under γ -ray irradiation [32]. There was no significant change observed in the lifetime of the glasses with the Ce^{3+} and Tm^{3+} ions. For a more detailed discussion, see Section 3.3.

3.2. Nature of point defects produced under irradiation

The carriers of the RE-doped fibers or glasses can be excited into trap states and subsequently form color centers in the glass matrix, which leads to RIA. Therefore, the RIA spectrum is an important parameter used to characterize the performance of radiation-resistant materials [8]. Additionally, EPR spectra are beneficial for identifying the nature of color centers. Considering the absorption of Tm^{2+} primarily occurs in the ultraviolet-visible (UV-Vis) region [33], one Tm^{3+} -free 1Al glass was prepared to eliminate the influence of the Tm^{3+} absorption on the deconvolution of the RIA spectra.

Fig. 4(a) presents the RIA spectrum of TAC aluminosilicate glasses after 1 kGy γ -ray irradiation. The RIA spectrum was obtained by subtracting the absorption of the original glasses from these irradiated glasses. One distinct absorption band at 540 nm was observed in the visible region. This can be derived from the point defects generated under irradiation. Compared to the glasses co-doped with Ce^{3+} , the TAC0 glass had the highest RIA level. In the visible region, the RIA intensity decreased significantly with an increase in $\text{Ce}^{3+}/\text{Tm}^{3+}$ ratio, which indicates that the radiation resistance of the TAC glasses can be obviously improved by doping with Ce^{3+} ions.

Fig. 4(b) shows the RIA spectrum of the Al^{3+} single-doped aluminosilicate glass (1Al), which decomposes the RIA spectrum into seven

Table 2

Peak position, full width at half maximum (FWHM) of the RIA spectra (in eV) and g values of the CW-EPR spectra of the various color centers in irradiated samples.

Type	Structural model	Absorption (± 0.1)	FWHM (± 0.1)	CW-EPR signal
Si-E'	$\equiv\text{Si}^{\bullet}$	5.8	0.8	yes
Al-E'	$\equiv\text{Al}^{\bullet}$	4.2	1.0	Not observed
POR	$\equiv\text{Si-O}\bullet$	4.8	0.6	yes
AlOHC	$\equiv\text{Al-O}^{\bullet}$	2.2 and 2.9	0.6 and 0.9	yes
AlODC	$=\text{Al}\cdot\text{R}=\text{}$	5.0	0.4	no

gaussian components with peaks at 2.14, 2.98, 4.16, 4.8, 5.0 and 5.81 eV and a tail extending from $>7\text{eV}$, respectively [34]. The cumulative fitted peak is in agreement with the actual measured RIA curves for the Al^{3+} single-doped aluminosilicate glass. These bands are attributed to the following centers:

- aluminum-oxygen hole center (AlOHC, a fourfold coordinated Al^{3+} with a hole trapped an oxygen atom, denoted as $\equiv\text{Al-O}^{\bullet}$, where “ \equiv ” represents bonds with three separate oxygen atoms [35]), (2.2 and 2.9 eV),
- aluminum dangling band (Al-E', an unpaired electron trapped in an Al^{3+} atom coordinated with three oxygen atoms, denoted as $\equiv\text{Al}^{\bullet}$) (4.2 eV), peroxy radical (POR, denoted as $\equiv\text{Si-O}\bullet$) (4.8 eV),
- aluminum oxygen deficiency center (AlODC, denoted as $\equiv\text{Al}\cdot\text{R}\equiv$) (5.1 eV) and
- silicon dangling band (Si-E', denoted as $\equiv\text{Si}^{\bullet}$) (5.8 eV) [36].

A similar result was reported by Hideo et al. [37].

Fig. 4(c) shows the first derivative EPR spectra of the irradiated TAC glasses. The strong axis characterized by $g = 2.001$ is attributed to the Si-E' center [36]. A sextet was observed which was assigned to AlOHC, due to the hyperfine interaction of the hole spin ($S = 1/2$) in one oxygen with the nuclear spin of ^{27}Al ($I = 5/2$, 100% abundant) [35,37]. Considering that the Al-E' has a longer spin lattice relaxation than Si-E' and AlOHC, it is only discernable in the dispersion mode (absorption mode in this work) and at very low microwave powers ($\sim\mu\text{W}$) [37,38]. Therefore, the Al-E' center was not detected in this work, even if they were present in irradiated Al^{3+} -containing aluminosilicate glass, as reported by Hosono and Hiroshi [37]. AlODC is an EPR silent center, which has been confirmed in a previous report [39]. For all glasses, the Si-E' and AlOHC

signal intensities decreased with an increase in the $\text{Ce}^{3+}/\text{Tm}^{3+}$ ratio. For glasses with a Ce_2O_3 content more than 0.06 mol%, the signal associated with the Al-related defects (AlOHC) nearly disappeared. (A detailed inhibition mechanism will be discussed in Section 3.3).

Table 2 summarizes the characteristic values of the color centers identified in the RIA and CW-EPR spectra. In this work, the parameters used in the RIA decomposition are quantitatively consistent with the data reported in Ref. [25], and each cumulative fitted spectrum is consistent with the experimental data.

3.3. Influence mechanism of Ce^{3+} -doping on radiation resistance and spectral properties

For clarity, we divide the following discussion into three parts: 1) the energy transfer mechanism in the near-infrared range before irradiation, 2) the energy transfer mechanism in the high-energy region before irradiation, and 3) the energy transfer mechanism after irradiation. We propose two hypotheses for the different possible Ce^{3+} influences in Tm^{3+} -doped aluminosilicate glasses before irradiation. The complexity of the discussion is due to the presence of both dopants (Ce^{3+} and Tm^{3+}) in addition to other ionization states (Ce^{4+} and Tm^{2+}) and color centers (Si-E' and AlOHC). Especially, the Ce^{3+} and Ce^{4+} redox processes are not well characterized in glasses. The first attempted assignment was reported by Lupi et al. [41] by using both the conduction and valency bands, the energy levels of dopants and traps of color centers with respect to these bands of the glass. Here, we provide additional details on the possible mechanisms that determine the effect of the $\text{Ce}^{3+}/\text{Tm}^{3+}$ ratio on the absorption, emission, and fluorescence lifetime before and after irradiation of the glasses under investigation, including the presence of Ce^{4+} cations and the nature of Si-E' and AlOHC color centers caused by irradiation.

3.3.1. Energy transfer mechanism limited in the near IR spectral range before irradiation

Fig. 5 displays the schematic diagram of the energy transfer mechanism among the Tm^{3+} , Ce^{3+} ions and color centers of the TAC aluminosilicate glasses limited to the near IR spectral range including an explanation of the color centers that suppress the 1800 nm emission. In the TAC0 glass, Tm^{3+} ions are initially excited from the ground state ($^3\text{H}_6$) to the excited state ($^3\text{H}_4$) under 808 nm excitation. The Tm^{3+} ions in the $^3\text{H}_4$ state transfers their energy to the $^3\text{F}_4$ level through a cross-relaxation (CR) process, which excites the $^3\text{F}_4 \rightarrow ^3\text{H}_6$ fluorescence around the 1800 nm emission. Owing to this CR process, the PL intensity

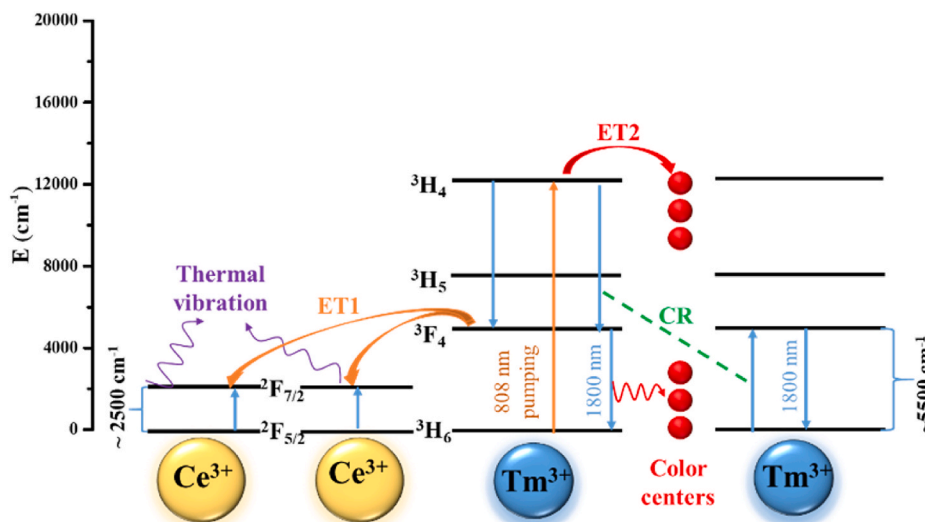


Fig. 5. Schematic diagram of the energy transfer mechanism limited to the near IR spectral range among Tm^{3+} , Ce^{3+} and color centers. ET: energy transfer, CR: cross-relaxation. (For interpretation of the references to color in this figure legend, the reader is referred to the Web version of this article.)

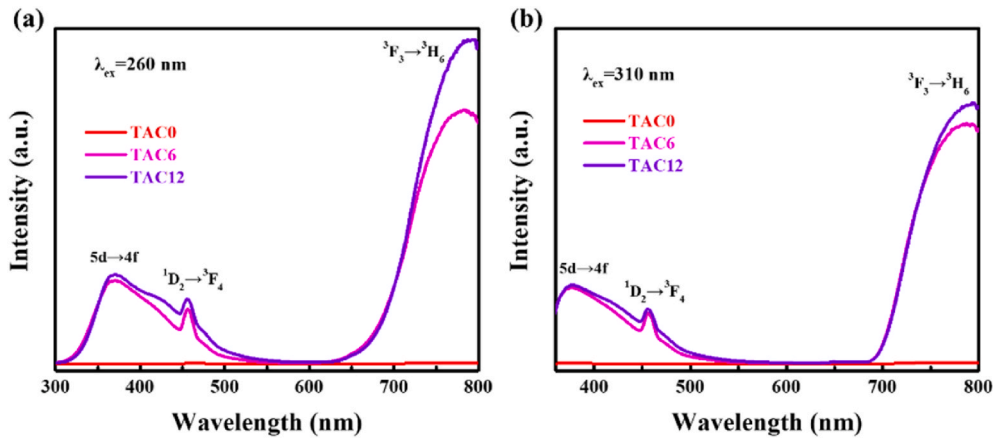


Fig. 6. Emission spectra of TAC0, TAC6 and TAC12 samples into UV radiations at both 260 nm (Ce^{4+} ions) and 310 nm (Ce^{3+} ions) at RT. We observe a Ce^{3+} 5d→4f broad band and some lines of Tm^{3+} ions, including $^1\text{D}_2 \rightarrow ^3\text{F}_4$ at 458 nm and $^3\text{F}_3 \rightarrow ^3\text{H}_6$ between 700 and 800 nm.

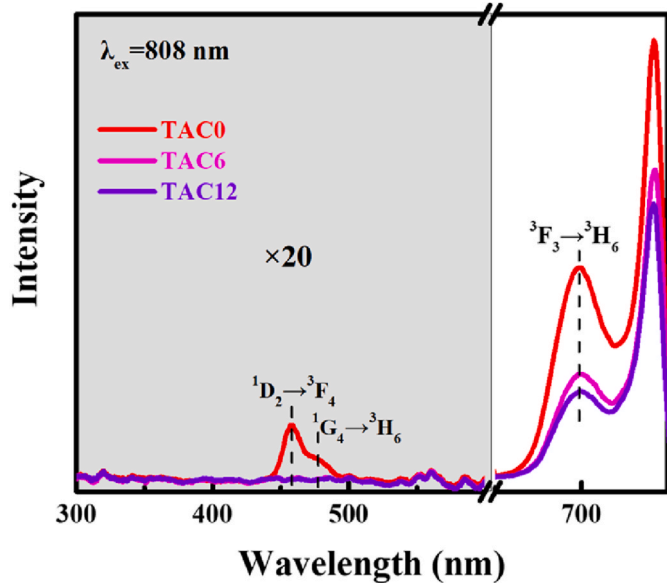


Fig. 7. Up-conversion emission spectra of $\text{Ce}^{3+}/\text{Tm}^{3+}$ -co-doped aluminosilicate glasses, measured under excitation of Tm^{3+} at $\lambda_{\text{ex}} = 808$ nm of laser diode.

at 1800 nm increased.

With the addition of Ce^{3+} ions, the energy may be transferred from the Tm^{3+} ion to the Ce^{3+} ions by cooperative down-conversion (ET1 process in Fig. 5), leading to non-radiative cooperative quenching. More precisely, the optical energy is simultaneously transferred from a single Tm^{3+} donor ion with an energy of $^3\text{F}_4 \rightarrow ^3\text{H}_6$ fluorescence (1800 nm of around 5555 cm^{-1}) simultaneously to a pair of Ce^{3+} acceptor ions ($\text{Tm}^{3+} \rightarrow 2\text{Ce}^{3+}$ cooperative acceptor) with twice lower $^2\text{F}_{5/2} \rightarrow ^2\text{F}_{7/2}$ transition energy of approximately $2000\text{--}2500 \text{ cm}^{-1}$. This cooperative down-conversion method was revealed by Basiev in $\text{Ce}^{3+}/\text{Tm}^{3+}$ -co-doped LaF_3 fluoride [31] as a consequence of the overlapping $^3\text{F}_4 \rightarrow ^3\text{H}_6$ luminescence broad line spectra of Tm^{3+} donor ions with the virtual absorption spectrum of two-particle acceptors obtained by the energy convolution of one-particle Ce^{3+} spectra. As shown in Ref. [31], the $^3\text{F}_4 \rightarrow ^3\text{H}_6$ transition of Tm^{3+} ion is in good resonance with the absorption of a cooperative pair acceptor (2Ce^{3+}), because the gap for the above-mentioned transitions is approximately twice as large as the energy of $^2\text{F}_{5/2} \rightarrow ^2\text{F}_{7/2}$ transition of Ce^{3+} ion. It should be noted that the $^2\text{F}_{5/2} \rightarrow ^2\text{F}_{7/2}$ transition of Ce^{3+} is located between 4 and $\sim 5 \mu\text{m}$ ($\sim 2000\text{--}2500 \text{ cm}^{-1}$), where the aluminosilicate glass is opaque.

Therefore, in aluminosilicate glasses, even with approximative overlapping of the energy transitions, these processes of low probability presumably occur so that the energy may be absorbed by the matrix, resulting in thermal vibrations. This results in a decrease in both the fluorescence intensity and lifetime of Tm^{3+} with an increase in the $\text{Ce}^{3+}/\text{Tm}^{3+}$ ratio in the glass before irradiation, as shown in Figs. 2 and 3.

3.3.2. Energy transfer mechanism limited in the high energy side before irradiation

The presence of Ce^{3+} ions was noted in Fig. 6 by pumping either Ce^{4+} ions at 260 nm or Ce^{3+} ions at 310 nm. The 5d→4f emission appears at approximately 360 nm by the addition of $5\text{d} \rightarrow ^2\text{F}_{5/2}$ and $5\text{d} \rightarrow ^2\text{F}_{7/2}$ broad bands. In addition, the Ce^{3+} - Tm^{3+} energy transfer is clearly seen by the $^1\text{D}_2 \rightarrow ^3\text{F}_4$ emission line at 458 nm and the $^3\text{F}_3 \rightarrow ^3\text{H}_6$ emission line between 700 and 800 nm.

Another explanation based on the up-conversion mechanism is proposed for the Tm^{3+} at 808 nm pumping. Owing to the absorption of multi-808 nm photons often observed in Tm^{3+} -doped crystals and glasses, higher levels such as $^1\text{D}_2$ can be reached. In the up-conversion emission spectra shown in Fig. 7, the weak $^1\text{D}_2 \rightarrow ^3\text{F}_4$ and $^1\text{G}_4 \rightarrow ^3\text{H}_6$ blue transitions of Tm^{3+} at approximately 458 nm and 476 nm were recorded solely in the TAC0 glass. The $^3\text{F}_3 \rightarrow ^3\text{H}_6$ transition of Tm^{3+} at approximately 700 nm decreased with increasing Ce^{3+} content. Therefore, even if the up-conversion efficiency in the aluminosilicate glass is relatively low owing to its high phonon energy ($\sim 1200 \text{ cm}^{-1}$), the observed up-conversion mechanism in Tm^{3+} ions can be described in Fig. 8. It is also possible that Tm^{3+} ions are excited to higher energy states while transferring energy to the 5d level of Ce^{3+} or the CT band of Ce^{4+} . However, the power density injected into the glass is low and decreases the population of high-energy particles below the detection threshold of the detector, which cannot capture the fluorescence signal. Thus, the 5d→4f transition fluorescence of Ce^{3+} , observed in the violet region as a broad band at approximately 360 nm in Fig. 8, was not detected in the up-conversion process of these aluminosilicate glasses under Tm^{3+} at 808 nm pumping. This detrimental effect also prevents the exploitation of laser emissions in the visible and near-infrared regions.

3.3.3. Energy transfer mechanism after irradiation

After high-energy irradiation of the TACO glass into the conduction band and higher energy bands, the radiation can ionize the precursor glass to generate the color center and a separate electron/hole. The electron or hole can be recombined by Tm^{3+} or other precursor centers, thus forming $\text{Tm}^{3+} \rightarrow \text{Tm}^{2+}$ or other electron/hole-trapping defects localized just below the conduction band [40]. A schematic

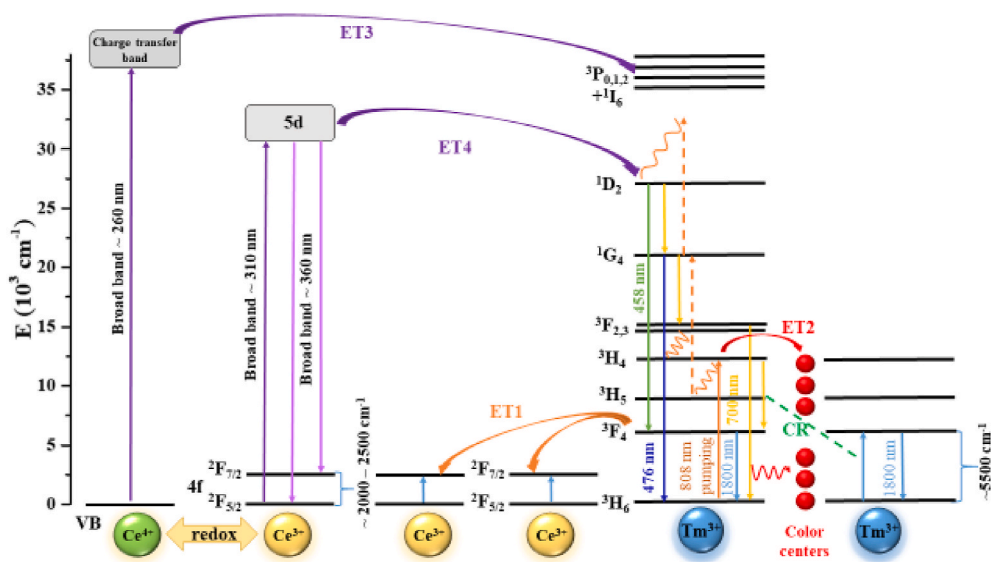


Fig. 8. Schematic diagram of energy transfer mechanisms after excitation into the high-energy side. ET: Energy transfer.

representation of the possible energy levels of dopants involved between valency and conduction bands has been detailed by Lupi [25]. The author analyzed the photodarkening process in thulium aluminosilicate fibers pumped at 1.07 μm and the quantitative effect of lanthanum, cerium, and thulium.

As shown in Fig. 4(a), radiation leads a strong RIA in the UV-VIS-NIR region, that covers the energy gap of ${}^3\text{H}_4$ – ${}^3\text{H}_6$. Thus, after relaxation between the highest and lowest Tm^{3+} energy levels, the defects might absorb the pump power and block the CR process, which triggers an energy transfer channel (ET2) from the Tm^{3+} ions to the color center (see Fig. 5). In addition to the role of the defect centers in the UV-VIS range, both the RIA in the NIR region and the reduction of Tm^{3+} to Tm^{2+} presumably decreased the PL intensity and lifetime of Tm^{3+} [14, 40].

For the $\text{Ce}^{3+}/\text{Tm}^{3+}$ -co-doped aluminosilicate glasses, there was minimal change in the luminescence lifetimes before and after irradiation. This implies that the formation of color centers is suppressed. It was proposed that the majority of cerium ions exist as Ce^{3+} which can be converted to Ce^{4+} ions by capturing radiation-induced holes and thereby decreases the concentration of trapped-hole centers (AIOHC) [25]. Meanwhile, Ce^{4+} can capture electrons and become Ce^{3+} , thus inhibiting the formation of trapped-electrons centers (Si-E'/Al-E') [41,42]. The Ce^{3+} and Ce^{4+} ions act as a buffer by releasing and capturing the holes and electrons to prevent glass damage during γ -ray irradiation.

4. Conclusions

In this study, the sol-gel method combined with the vacuum sintering method was used to prepare $\text{Ce}^{3+}/\text{Tm}^{3+}$ -co-doped aluminosilicate glasses with different $\text{Ce}^{3+}/\text{Tm}^{3+}$ ratios. The results show that the radiation resistance is positively related to the $\text{Ce}^{3+}/\text{Tm}^{3+}$ ratio. However, the spectral properties of Tm^{3+} ions deteriorate when the $\text{Ce}^{3+}/\text{Tm}^{3+}$ molar ratio exceeds 0.3. Before irradiation, as the $\text{Ce}^{3+}/\text{Tm}^{3+}$ ratio increased from 0 to 1.2, the PL intensity of Tm^{3+} ions and the fluorescence lifetime decreased by 30 and 21% respectively (438 μs –346 μs). After irradiation, a distinct decrease in PL intensity and fluorescence lifetime (from 438 μs to 376 μs) was observed for the TAC0 glass without Ce^{3+} -doping, while the changes were inconsequential for the TAC glass with a $\text{Ce}^{3+}/\text{Tm}^{3+}$ ratio greater than 0.3. The nature of Si-E' and AIOHC color centers caused by irradiation was identified by RIA and EPR spectroscopies.

By simultaneously considering the spectral properties and radiation resistance of the glass, the optimal $\text{Ce}^{3+}/\text{Tm}^{3+}$ molar ratio suggested for

radiation-resistant Tm^{3+} -doped aluminosilicate fibers used in harsh irradiation environments is <0.3. Before and after irradiation, Ce^{3+} and Ce^{4+} ions act as buffer agents by releasing and capturing the holes and electrons to prevent glass damage during γ -ray irradiation.

Authorship contribution statement

Yan Jiao: Writing - original draft, Formal analysis, review & editing. Chongyun Shao: Conceptualization, Writing - review. Mengting Guo: Properties testing and discussion. Malgorzata Guzik: Writing - review. Yang Zhang: Investigation. Chunlei Yu: Resources, Funding acquisition. Georges Boulon: Conceptualization, Writing - review. Lili Hu: Resources, Funding acquisition, Supervision, Writing - review.

CRediT authorship contribution statement

Yan Jiao: Writing - original draft, Formal analysis, review & editing. Chongyun Shao: Conceptualization, Writing - review. Mengting Guo: Properties testing and discussion. Malgorzata Guzik: Writing - review. Yang Zhang: Investigation. Chunlei Yu: Resources, Funding acquisition. Georges Boulon: Conceptualization, Writing - review. Lili Hu: Resources, Funding acquisition, Supervision, Writing - review.

Declaration of competing interest

The authors declare that they have no known competing financial interests or personal relationships that could have appeared to influence the work reported in this paper.

Acknowledgement

This work is supported by the National Natural Science Foundation of China (Grant Nos. 62005297 and 61875216).

References

- [1] Z. Zheng, D. Ouyang, X. Ren, J. Wang, J. Pei, S. Ruan, 0.33 mJ, 104.3 W dissipative soliton resonance based on a figure-of-9 double-clad Tm-doped oscillator and an all-fiber MOPA system, *Photon. Res.* 7 (2019) 513–517, <https://doi.org/10.1364/PRJ.7.000513>.
- [2] N.P. Barnes, B.M. Walsh, D.J. Reichle, R.J. DeYoung, Tm: fiber lasers for remote sensing, *Opt. Mater.* 31 (2009) 1061–1064, <https://doi.org/10.1016/j.optmat.2007.11.037>.

- [3] Z. Li, A. Heidt, J. Daniel, Y. Jung, S. Alam, D.J. Richardson, Thulium-doped fiber amplifier for optical communications at 2 μm , *Opt Express* 21 (2013) 9289–9297, <https://doi.org/10.1364/OE.21.009289>.
- [4] E. Ji, J. Shi, C. Zha, J. Zeng, X. Zhou, Z. He, Y. Yao, Q. Lü, Ultimate capacity analysis of cladding-pumped 10/130 Tm: fiber laser, *Chin. Opt Lett.* 18 (2020) 51404, <https://doi.org/10.3788/COL202018.051404>.
- [5] M. Juárez-Hernández, E.J.C.O.L. Mejía, Spectral analysis of short-wavelength emission by up-conversion in a Tm 3+: ZBLAN dual-diode-pumped optical fiber, *Chin. Opt Lett.* 18 (2020) 71901, <https://doi.org/10.3788/COL202018.071901>.
- [6] S.D. Jackson, Towards high-power mid-infrared emission from a fibre laser, *Nat. Photonics* 6 (2012) 423, <https://doi.org/10.1038/nphoton.2012.149>.
- [7] J. Zhao, L. Li, L. Zhao, D. Tang, D. Shen, L.J.P.R. Su, Tunable and switchable harmonic h-shaped pulse generation in a 3.03 km ultralong mode-locked thulium-doped fiber laser, *Photon. Res.* 7 (2019) 332–340, <https://doi.org/10.1364/PRJ.7.000332>.
- [8] S. Girard, B. Torteche, E. Regnier, M. Van Uffelen, A. Gusarov, Y. Ouerdane, J. Baggio, P. Paillot, V. Ferlet-Cavrois, A. Boukenter, Proton-and gamma-induced effects on erbium-doped optical fibers, *IEEE Trans. Nucl. Sci.* 54 (2007) 2426–2434, <https://doi.org/10.1109/TNS.2007.910859>.
- [9] S. Wang, F. Lou, C. Yu, Q. Zhou, M. Wang, S. Feng, D. Chen, L. Hu, W. Chen, M. Guzik, G. Boulon, Influence of Al³⁺ and P⁵⁺ ion contents on the valence state of Yb³⁺ ions and the dispersion effect of Al³⁺ and P⁵⁺ ions on Yb³⁺ ions in silica glass, *J. Mater. Chem. C* 2 (2014) 4406–4414, <https://doi.org/10.1039/c3tc32576h>.
- [10] D. Griscom, M. Gingerich, E. Friebele, Radiation-induced defects in glasses: origin of power-law dependence of concentration on dose, *Phys. Rev. Lett.* 71 (1993) 1019, <https://doi.org/10.1103/PhysRevLett.71.1019>.
- [11] T. Deschamps, H. Vezin, C. Gonnet, N. Ollier, Evidence of AIOHC responsible for the radiation-induced darkening in Yb doped fiber, *Opt Express* 21 (2013) 8382–8392, <https://doi.org/10.1364/OE.21.008382>.
- [12] G. Origlio, F. Messina, S. Girard, M. Cannas, A. Boukenter, Y. Ouerdane, Spectroscopic studies of the origin of radiation-induced degradation in phosphorus-doped optical fibers and preforms, *J. Appl. Phys.* 108 (2010) 123103, <https://doi.org/10.1063/1.3517479>.
- [13] M. Lezius, K. Predehl, W. Stower, A. Turler, M. Greiter, C. Hoeschen, P. Thirof, W. Assmann, D. Habs, A. Prokofiev, Radiation induced absorption in rare earth doped optical fibers, *IEEE Trans. Nucl. Sci.* 59 (2012) 425–433, <https://doi.org/10.1109/TNS.2011.2178862>.
- [14] S. Girard, A. Alessi, N. Richard, L. Martin-Samos, V. De Michele, L. Giacomazzi, S. Agnello, D. Di Francesca, A. Morana, B.J.R.I.P. Winkler, Overview of radiation induced point defects in silica-based optical fibers, *Rev. Phys.* 4 (2019) 100032, <https://doi.org/10.1016/j.revip.2019.100032>.
- [15] Y. Xing, Y. Liu, N. Zhao, R. Cao, Y. Wang, Y. Yang, J. Peng, H. Li, L. Yang, N. Dai, Radical passive bleaching of Tm-doped silica fiber with deuterium, *Opt. Lett.* 43 (2018) 1075–1078, <https://doi.org/10.1364/OL.43.001075>.
- [16] M. Vivona, S. Girard, C. Marcandella, T. Robin, B. Cadier, M. Cannas, A. Boukenter, Y. Ouerdane, Influence of Ce codoping and H₂ pre-loading on Er/Yb-doped fiber: radiation response characterized by confocal micro-luminescence, *J. Non-Cryst. Solids* 357 (2011) 1963–1965, <https://doi.org/10.1016/j.jnoncrysol.2010.10.039>.
- [17] R. Cao, G. Chen, Y. Chen, Z. Zhang, X. Lin, B. Dai, L. Yang, J. Li, Effective suppression of the photodarkening effect in high-power Yb-doped fiber amplifiers by H₂ loading, *Photon. Res.* 8 (2020) 288–295, <https://doi.org/10.1364/PRJ.381208>.
- [18] E.J. Friebele, M.E. Gingerich, Photobleaching effects in optical fiber waveguides, *Appl. Opt.* 20 (1981) 3448–3452, <https://doi.org/10.1364/AO.20.003448>.
- [19] S. Girard, A. Laurent, E. Pinsard, T. Robin, B. Cadier, M. Boutillier, C. Marcandella, A. Boukenter, Y.J.O.L. Ouerdane, Radiation-hard erbium optical fiber and fiber amplifier for both low-and high-dose space missions, *Opt. Lett.* 39 (2014) 2541–2544, <https://doi.org/10.1364/OL.39.002541>.
- [20] C. Shao, Y. Jiao, F. Lou, M. Wang, L. Zhang, S. Feng, S. Wang, D. Chen, C. Yu, L. Hu, Enhanced radiation resistance of ytterbium-doped silica fiber by pretreating on a fiber preform, *Opt. Mater. Express* 10 (2020) 408–420, <https://doi.org/10.1364/OME.384362>.
- [21] E. Friebele, D.L. Griscom, Color Centers in Glass Optical Fiber Waveguides, MRS Online Proceedings Library Archive, 1985, <https://doi.org/10.1557/PROC-61-319>, 61.
- [22] Y. Xing, Y. Liu, R. Cao, L. Liao, Y. Chu, Y. Wang, J. Peng, H. Li, L. Yang, N. Dai, Elimination of radiation damage in Tm-doped silica fibers based on the radical bleaching of deuterium loading, *OSA Continuum* 1 (2018) 987–995, <https://doi.org/10.1364/OSAC.1.000987>.
- [23] Y. Xing, N. Zhao, L. Liao, Y. Wang, H. Li, J. Peng, L. Yang, N. Dai, J. Li, Active radiation hardening of Tm-doped silica fiber based on pump bleaching, *Opt Express* 23 (2015) 24236–24245, <https://doi.org/10.1364/OE.23.024236>.
- [24] S. Girard, M. Vivona, A. Laurent, B. Cadier, C. Marcandella, T. Robin, E. Pinsard, A. Boukenter, Y. Ouerdane, Radiation hardening techniques for Er/Yb doped optical fibers and amplifiers for space application, *Opt Express* 20 (2012) 8457–8465, <https://doi.org/10.1364/OE.20.008457>.
- [25] C. Shao, W. Xu, N. Ollier, M. Guzik, G. Boulon, L. Yu, L. Zhang, C. Yu, S. Wang, L. Hu, Suppression mechanism of radiation-induced darkening by Ce doping in Al/Yb/Ce-doped silica glasses: evidence from optical spectroscopy, EPR and XPS analyses, *J. Appl. Phys.* 120 (2016) 153101, <https://doi.org/10.1063/1.4964878>.
- [26] S. Baccaro, A. Cecilia, E. Mihokova, M. Nikl, K. Nitsch, P. Polato, G. Zanella, R. Zannoni, Radiation damage induced by γ irradiation on Ce³⁺ doped phosphate and silicate scintillating glasses, *J. Nucl. Instrum. Meth. A* 476 (2002) 785–789, [https://doi.org/10.1016/S0168-9002\(01\)01676-X](https://doi.org/10.1016/S0168-9002(01)01676-X).
- [27] S. Liu, H. Li, Y. Tang, L. Hu, Fabrication and spectroscopic properties of Yb³⁺-doped silica glasses using the sol-gel method, *Chin. Opt Lett.* 10 (2012) 81601, <https://doi.org/10.3788/COL201210.081601>.
- [28] M. Engholm, P. Jelger, F. Laurell, L. Norin, Improved photodarkening resistivity in ytterbium-doped fiber lasers by cerium codoping, *Opt. Lett.* 34 (2009) 1285–1287, <https://doi.org/10.1364/OL.34.001285>.
- [29] G. Dantelle, G. Boulon, Y. Guyot, D. Testemale, M. Guzik, S. Kurosawa, K. Kamada, A. Yoshikawa, Research on efficient fast scintillators: evidence and X-ray absorption near edge spectroscopy characterization of Ce⁴⁺ in Ce³⁺, Mg²⁺-Co-doped Gd₃Al₂Ga₃O₁₂ garnet crystal, *Phys. Status Solidi B-Basic Solid* 257 (2020) 1900510, <https://doi.org/10.1002/psb.201900510>.
- [30] S. Blahuta, A. Bessiere, B. Viana, P. Dorenbos, V. Ouspenski, Evidence and consequences of Ce⁴⁺ in LYSO: Ce, Ca and LYSO: Ce, Mg single crystals for medical imaging applications, *IEEE Trans. Nucl. Sci.* 60 (2013) 3134–3141, <https://doi.org/10.1109/TNS.2013.2269700>.
- [31] T. Basiev, M. Doroshenko, V. Osiko, A. Prokhorov, Highly efficient cooperative energy transfer from Ho³⁺ and Tm³⁺ ions to Ce³⁺ ions in crystals, *J. Exp. Theor. Phys.* 93 (2001) 1178–1183, <https://doi.org/10.1134/1.1435738>.
- [32] V. Pukhkaya, P. Goldner, A. Ferrier, N. Ollier, Impact of rare earth element clusters on the excited state lifetime evolution under irradiation in oxide glasses, *Opt Express* 23 (2015) 3270–3281, <https://doi.org/10.1364/OE.23.003270>.
- [33] J. Sils, S. Hausfeld, W. Clauß, U. Pahl, R. Lindner, M. Reichling, Impurities in synthetic fluorite for deep ultraviolet optical applications, *J. Appl. Phys.* 106 (2009), <https://doi.org/10.1063/1.3224879>.
- [34] C. Shao, M. Guo, Y. Zhang, L. Zhou, M. Guzik, G. Boulon, C. Yu, D. Chen, L. Hu, 193 nm excimer laser-induced color centers in Yb³⁺/Al³⁺/P⁵⁺-doped silica glasses, *J. Non-Cryst. Solids* 544 (2020) 120198, <https://doi.org/10.1016/j.jnoncrysol.2020.120198>.
- [35] J.C. Lagomacini, D. Bravo, A. Martín, F.J. López, P. Martín, Á. Ibarra, Growth kinetics of AIOHC defects in γ -irradiated silica glasses, *J. Non-Cryst. Solids* 403 (2014) 5–8, <https://doi.org/10.1016/j.jnoncrysol.2014.04.005>.
- [36] D.L. Griscom, E' center in glassy SiO₂: microwave saturation properties and confirmation of the primary ²⁹Si hyperfine structure, *Phys. Rev. B* 20 (1979) 1823, <https://doi.org/10.1103/PhysRevB.20.1823>.
- [37] H. Hideo, K. Hiroshi, Radiation-induced coloring and paramagnetic centers in synthetic SiO₂: Al glasses, *Nucl. Instrum. Methods B* 91 (1994) 395–399, [https://doi.org/10.1016/0168-583X\(94\)96255-3](https://doi.org/10.1016/0168-583X(94)96255-3).
- [38] K. Brower, Electron paramagnetic resonance of Al-E' centers in vitreous silica, *Phys. Rev. B* 20 (1979) 1799, <https://doi.org/10.1103/PhysRevB.20.1799>.
- [39] H. Imai, K. Arai, H. Imagawa, H. Hosono, Y.J.P.R.B. Abe, Two types of oxygen-deficient centers in synthetic silica glass, *Phys. Rev. B* 38 (1988) 12772, <https://doi.org/10.1103/PhysRevB.38.12772>.
- [40] Y. Xing, F. Zhang, Y. Chen, Y. Wang, Y. Liu, H. Li, J. Peng, L. Yang, N. Dai, J. Li, The influence of Thulium impurity on photobleaching in a photodarkened ytterbium-doped silica double-cladding fiber, *Laser Phys. Lett.* 16 (2019) 65104, <https://doi.org/10.1088/1612-202X/ab1920>.
- [41] J. Lupi, M. Vermillac, W. Blanc, F. Mady, M. Benabdesselam, B. Dussardier, D. Neuville, Steady photodarkening of thulium aluminosilicate fibers pumped at 1.07 μm : quantitative effect of lanthanum, cerium, and thulium, *Opt. Lett.* 41 (2016) 2771–2774, <https://doi.org/10.1364/OL.41.002771>.
- [42] F. Mady, A. Guttilla, M. Benabdesselam, W. Blanc, Systematic investigation of composition effects on the radiation-induced attenuation mechanisms of aluminosilicate, Yb-doped silicate, Yb-and Yb, Ce-doped aluminosilicate fiber preforms, *Opt. Mater. Express* 9 (2019) 2466–2489, <https://doi.org/10.1364/OME.9.002466>.